

Activating mutations in *BRAF* characterize a spectrum of pediatric low-grade gliomas

Margaret J. Dougherty, Mariarita Santi, Marcia S. Brose, Changqing Ma, Adam C. Resnick, Angela J. Sievert, Phillip B. Storm, and Jaclyn A. Biegel

Departments of Pediatrics (M.J.D., A.J.S., J.A.B.); Pathology (M.S., J.A.B.); Medicine (M.S.B.); Otorhinolaryngology (M.S.B., C.M.); and Neurosurgery (A.C.R., P.B.S.), The Children's Hospital of Philadelphia and the University of Pennsylvania School of Medicine, Philadelphia, Pennsylvania

In the present study, DNA from 27 grade I and grade II pediatric gliomas, including ganglioglioma, desmoplastic infantile ganglioglioma, dysembryoplastic neuroepithelial tumor, and pleomorphic xanthoastrocytoma was analyzed using the Illumina 610K Beadchip SNP-based oligonucleotide array. Several consistent abnormalities, including gain of chromosome 7 and loss of 9p21 were observed. Based on our previous studies, in which we demonstrated *BRAF* mutations in 3 gangliogliomas, 31 tumors were screened for activating mutations in exons 11 and 15 of the *BRAF* oncogene or a *KIAA1549-BRAF* fusion product. There were no cases with a *KIAA1549-BRAF* fusion. A *BRAF* V600E mutation was detected in 14 of 31 tumors, which was not correlated with any consistent pattern of aberrations detected by the SNP array analysis. Tumors were also screened for mutations in codon 132 in exon 4 of *IDH1*, exons 2 and 3 of *KRAS*, and exons 2–9 of *TP53*. No mutations in *KRAS* or *TP53* were identified in any of the samples, and there was only 1 *IDH1* R132H mutation detected among the sample set. *BRAF* mutations constitute a major genetic alteration in this histologic group of pediatric brain tumors and may serve as a molecular target for biologically based inhibitors.

Keywords: *BRAF*, desmoplastic infantile ganglioglioma, dysembryoplastic neuroepithelial tumor, ganglioglioma, pleomorphic xanthoastrocytoma, SNP array.

Low-grade gliomas represent the most common group of brain tumors in children and are composed of a variety of histologic entities classified

by the World Health Organization as grade I and grade II neoplasms.¹ The most common type is pilocytic astrocytoma, which accounts for approximately 20% of pediatric brain tumors. A spectrum of mixed glial and neuronal tumors of childhood, including ganglioglioma (GG) and pleomorphic xanthoastrocytoma (PXA), may each only comprise 0.5%–1% of central nervous system tumors in the first decades of life. The molecular etiology for the majority of these tumors has been difficult to elucidate, despite the application of a variety of genome-wide and candidate gene approaches. We and others recently described a tandem duplication in chromosome band 7q34 that results in a *KIAA1549-BRAF* fusion and constitutive activation of *BRAF* in the majority of pilocytic astrocytomas, as well as a limited number of fibrillary (grade II) astrocytomas.^{2–4} *BRAF* is a member of the RAF family of serine/threonine protein kinases and is a key intermediary in the RAS-RAF-MEK-ERK-MAP kinase signaling pathway. This pathway is implicated in a wide variety of cellular functions, including cell proliferation, cell-cycle arrest, terminal differentiation, and apoptosis.⁵ Activating mutations in *BRAF* have been implicated in approximately 66% of melanomas, in a smaller percentage of thyroid, colonic, and ovarian carcinomas, in some sarcomas^{6,7} and in a limited number of malignant gliomas. A single amino acid substitution in exon 15 at residue 600 results in constitutive activation of the *BRAF* kinase function and accounts for the majority of *BRAF* mutations. Mutations in exon 11 are seen less frequently.⁶ We initially identified a *BRAF* V600E mutation in 3 of 11 pediatric GGs, suggesting that the MAPK pathway may be activated in a number of different histologic subtypes of brain tumors.²

Germline mutations in the *BRAF* gene have also been described in cardio-facio-cutaneous (CFC) syndrome, one of a number of genetic disorders that, similar to NF1, results from abnormalities in altered ERK pathway signaling. In addition to *BRAF*, mutations in *KRAS*, *PTPN11*, *MEK1/2*, and *HRAS* have been

Received May 15, 2009; accepted November 25, 2009.

Corresponding Author: Jaclyn A. Biegel, PhD, The Children's Hospital of Philadelphia, Room 1002 Abramson Research Building, 3615 Civic Center Boulevard, Philadelphia, PA 19104 (biegel@mail.med.upenn.edu).

documented in CFC, Noonan, Costello, and LEOPARD syndromes.⁸ Patients with these disorders typically have some combination of facial abnormalities, heart defects, and short stature. Skin and genital abnormalities and mental retardation are also common phenotypes in patients with these disorders. As in NF1, patients may be predisposed to cancer, including rhabdomyosarcoma in Costello syndrome⁹ and juvenile myelomonocytic leukemia in Noonan syndrome.¹⁰ Patients with germline *BRAF* mutations and glioma have not yet been reported.

Gangliocytoma/ganglioglioma, desmoplastic infantile astrocytoma/ganglioglioma (DIA/DIG), dysembryoplastic neuroepithelial tumor (DNT), PXA, and pilocytic astrocytoma (PA) are all well-recognized, low-grade neuroepithelial tumors, characterized by a neoplastic glial component with fairly distinct histological features and a variable amount of ganglion or neuronal elements.¹ Overlapping histologic features can make the differential diagnosis difficult in some cases. Virtually all DIGs occur in patients under the age of 2 years. DNT, GG, and PXA have a much wider age range, from early infancy to late adulthood. The tumors are mostly supratentorial with a predilection for the temporal lobe. Most patients have a history of seizures as the main presenting feature. Although all of these tumors are relatively benign, prognosis often depends on location and the ability to achieve a complete surgical resection. While PXA or GG are more likely to undergo malignant transformation,¹¹ tumors that progress may require further treatment with radiation and/or chemotherapy.

The histopathologic hallmark of GG is a combination of neoplastic ganglion/neuronal cells and neoplastic glial cells with features ranging from fibrillary astrocytoma to oligodendroglioma or PA. Even typical PAs may occasionally contain neurons that appear to be part of the neoplasm, and tumors may be classified as GG with prominent PA, or PA with a prominent neuronal component.¹¹ Rare lesions with distinct components of DNT and conventional GG (composite tumors) have also been reported.^{12–15}

Overlapping histologic, clinical, and radiographic characteristics for GG, PXA, DIA/DIG, and DNT highlight the difficulty in providing an accurate differential diagnosis, and it is rarely possible to prospectively identify which tumors have a high likelihood of progression. Understanding common vs. distinct biologic pathways that lead to the initial abnormal growth and subsequent malignant transformation of these neoplasms could provide an alternative means of classification, which could be used for risk stratification and treatment.

Towards this aim, recent studies using array comparative genomic hybridization (aCGH) have identified several non-random genomic aberrations in GG.^{16–18} The most common aberrations identified were gain of chromosomes 5, 7, 8, and 12 and loss of chromosomes 9, 10, and 22.¹⁷ Interphase FISH demonstrated several abnormalities associated with malignant gliomas (CDK4 amplification, loss of the tumor suppressor genes *CDKN2A/B* and *DMBT1*) that were present in the glial cell component but were not observed in the

neuronal cells of these tumors.¹⁷ The specific identification of these abnormalities in tumors that progressed to anaplastic GG raises the possibility of their clinical utility as prognostic markers.

Less is known about the molecular etiology of PXA, DNT, and DIG. Cytogenetic abnormalities seen in more than 1 PXA have included gain of chromosomes 3, 4, 5, 7, 19, 20, and X, and loss of chromosomes 8, 9, 17, 18, 20, and 22.^{19,20} Weber et al.²¹ reported a homozygous deletion of 9p21.3, which includes *CDKN2A*, in 60% of PXAs.²¹ Forshev et al.⁴ reported 1 PXA with loss of 9p21, gain of 7, and a V600E *BRAF* mutation. Case reports describing cytogenetic analysis or aCGH analysis of DIG^{22,23} and DNT²⁴ have demonstrated normal profiles as well as hypotetraploid cells with numerous abnormalities.

Candidate gene approaches have also yielded little information on the molecular etiology of these tumors. The tuberous sclerosis genes, *TSC1* and *TSC2*, may play a role in a subset of GG.^{25,26} Mutations in *IDH1* have been reported in 68%–82% of grade II astrocytic and oligodendroglial tumors in adults.^{27–30} Studies performed on limited numbers of pediatric glioblastomas indicate that *IDH1* mutations are infrequent in these tumors.^{27,30} A case study of a GG with areas of malignant transformation showed overexpression of p53 and a mutation in exon 7 of *TP53* in the malignant component of the tumor, but no p53 immunoreactivity or *TP53* mutations in exons 5–8 in the benign GG.¹⁸ Pollack et al.³¹ showed a strong association between overexpression of p53 or *TP53* mutation and adverse prognosis in pediatric patients with malignant gliomas, but *TP53* mutations in sporadic low-grade gliomas in children are not seen.³² Mutations in *BRAF*, *KRAS*, and *NRAS* have been identified in 1%–4% of malignant gliomas, primarily in adults.^{33–35}

The aim of the present study was to explore the prevalence of *BRAF* duplications or mutation in a spectrum of mixed glial and neuronal low-grade gliomas in children, as well as to identify additional non-random genomic alterations that might pinpoint other genes or pathways of interest.

Materials and Methods

Tissue Specimens

Twenty-nine of the 33 specimens analyzed in the present study were obtained from patients undergoing tumor resection at The Children's Hospital of Philadelphia (CHOP). Two of the 4 specimens from outside institutions (04-119 and 06-232B) have been previously described.^{36,37} Informed consent was obtained as per an Institutional Review Board approved protocol and cases were assigned a tumor bank number. Diagnosis was confirmed by pathology review. In addition, INI1 immunohistochemistry (IHC) was performed on any samples that had a loss of chromosome 22 by array analysis. The 33 specimens included 12 GGs, 5 GGs with a prominent astrocytic component, 1 GG with an anaplastic glial

component, 1 glioblastoma multiforme (GBM) arising in the setting of a GG, 1 atypical teratoid/rhabdoid tumor (AT/RT) evolving from a GG, 2 GG/DNT, 3 DNTs, 2 DIGs, 3 PXAs, 1 PXA with neuronal differentiation, and 2 AT/RTs evolving from PXAs. With the exception of case 04-119, all tumors were obtained at initial diagnosis with no prior exposure to chemotherapy or radiation. Twenty-seven of the samples obtained from CHOP were snap frozen in liquid nitrogen and stored at -80°C for DNA and RNA extraction. Samples 04-119, 06-232B, 08-308B, 09-47, 09-48, and 09-78 were received as formalin-fixed paraffin-embedded tissue. DNA and RNA were extracted from tissue and available peripheral blood specimens and cDNA was synthesized as previously described.²

Illumina SNP Array Analysis

The Infinium II assay was performed using the Illumina HumanHap610 genotyping BeadChip array (594,906 SNPs and copy number markers analyzed) according to the manufacturer's specifications (Illumina) by the Center for Applied Genomics at CHOP. The specific details have been reported.^{2,38,39} Two parameters, the \log_2R ratio and the B allele frequency, provide information regarding copy number and genotype, respectively, and were determined by visual inspection of BeadStudio files. Copy number alterations (CNAs) <10 SNPs in size and copy number neutral loss of heterozygosity (CN LOH) events <5 Mb in size were excluded from analysis. Results were compared with an in-house database of known, common copy number variations seen in healthy controls. All genomic positions were based upon hg18 (March, 2006) from the UCSC Genome Browser (<http://genome.ucsc.edu/>).

PCR and Sequence Analysis

Primers for exons 11 and 15 of the *BRAF* gene have been described.⁶ RT-PCR primers for the *KIAA1549-BRAF* fusion gene were previously reported.² Genomic PCR primers for the *KIAA1549-BRAF* fusion gene were designed in the introns of *KIAA1549* and *BRAF*. The sense primer gKIAA-4F, CTCTCTCTAAGTGGCAATGTAATGCTGA, is located in intron 16 of *KIAA1549*. The antisense primer gBRAF-3R, AGATGCACACA TTGGAAGTAAGTGAAAA, is located in intron 8 of *BRAF*. Primers for exon 4 of *IDH1*, exons 2 and 3 of *KRAS*, and exons 2–9 of *TP53* have been described.^{27–29,40–42} Sequencing of PCR products was performed using the BigDye Terminator v3.1 Cycle Sequencing Kit from Applied Biosystems as per the manufacturer's protocol. Sequencing products were analyzed on a 3730 DNA Analyzer (Applied Biosystems) by the CHOP Nucleic Acid/Protein Core.

Immunohistochemistry

Immunohistochemistry assays for phosphorylated ERK protein (phospho-ERK) were performed on $5\ \mu\text{m}$

sections of formalin-fixed paraffin-embedded (FFPE) tissue according to the manufacturer's recommendations. Briefly, sections were incubated at 70°C overnight, de-paraffinized with xylene (15 minutes twice), rinsed with 100% ethanol, and then rehydrated with 95% ethanol and water. Antigen unmasking was subsequently done with a citrate-based solution from Vector Laboratories at above 98°C for 20 minutes. Endogenous peroxidase activity was blocked by 3% hydrogen peroxide at room temperature for 15 minutes and sections were washed with $1\times$ PBS/0.1% Tween-20 ($1\times$ PBST). Sections were then incubated with 5% normal goat serum in $1\times$ PBST for an hour to block any nonspecific binding, followed by incubation with anti-human phospho-ERK (Thr 202/Tyr204) antibody (Cell Signaling; Catalog number: 4370) at 1:400 dilution overnight at 4°C . Following washing, sections were incubated with biotinylated goat anti-rabbit IgG (1:200) for 30 minutes at room temperature, washed, and incubated with Avidin: Biotinylated enzyme Complex (ABC, Vectastain Elite ABC Kit from Vector Laboratories) at room temperature for 30 minutes. Bound antibody was visualized by 3, 3'-Diaminobenzidine (DAB, Vector Laboratories).

Immunohistochemistry for p53 (DO-7, Dako) was performed on $4\ \mu\text{m}$ thick, FFPE tissue sections, using Autostainer Link 48 (Dako). The antibody was used at 1:100 dilution and pressure cooker (Biomedical) antigen retrieval was performed. The EnVision Flex Kit (Dako) was used for antigen retrieval, pretreatment condition, and detection. The sections were counterstained with Gill's hematoxylin, washed, dehydrated with graded concentrations of ethanol, cleared in xylene, mounted, and examined microscopically. Appropriate positive and negative control samples were used. Cells with dense nuclear staining were interpreted as positive. Tumors were categorized as expressing little or no p53 (grade 0 or 1) or as positive for p53 with staining present in a sizable subgroup of cells (25 to 50 percent; grade 2), most cells (50%–75%; grade 3) or nearly all cells ($>75\%$; grade 4) in the high-power fields in areas with maximal staining. Positivity was therefore defined semiquantitatively, based on the percentage of p53 expressing cells in the tumor.³¹

Results

The clinical demographics for the 33 patients are shown in Table 1. Patients ranged in age from 10 months to 36 years old, and there were 17 males and 16 females. The results of the SNP array analyses for 27 tumors and *BRAF* mutation status for the 31 tumors with adequate DNA are shown in Table 2. Representative array results are shown in Fig. 1. As shown in Table 2, the number of gains per tumor sample ranged from 0 to 12. The number of losses per tumor sample ranged from 0 to 6, with the exception of case 95-56, which demonstrated 11 losses and 21 gains. CNAs seen in more than 1 tumor included gain of chromosome 7, heterozygous loss of

Table 1. Clinical demographics for the 33 patients

Case	Age	Sex	Diagnosis	Location
00-317	17y	M	GG	L-parietal
00-352	1y11m	F	GG	L-cerebellar
01-29	17y	M	GG	R-occipital
02-145	5y	M	GG	R-paracentral
03-126	11y	F	GG	R-temporal
04-168	11y	M	GG	Cerebellum
05-97	12y	F	GG	Temporal
07-304	13y	M	GG	R-frontal
07-350	11y	F	GG	R-temporal
08-113	16y	F	GG	R-temporal
08-247	15y	F	GG	L-temporal
09-127	5y	F	GG	R-temporal
00-301	17y	M	GG with prominent pilocytic astrocytoma	Cerebellum
02-03	5y	M	GG with prominent astrocytic component	L-temporal
04-234	17y	F	GG with prominent astrocytic component	R-parietal
05-22	17y	F	GG with prominent astrocytic component	R-parietal
06-91	16y	F	GG with prominent astrocytic component	Cerebellum
05-253	9y	M	GG with anaplastic glial component	L-parietal
06-107	8y	M	GBM arising in a GG	Intrinsic pontine
04-119	11y	M	AT/RT evolving from a GG	Optic pathway
00-358	5y	M	GG/DNT	L-frontal
01-44	11y	M	GG/DNT	L-occipital
95-56	13y	M	DNT	R-temporal
01-206	9y	M	DNT	R-temporal
05-137	16y	M	DNT	L-temporal
06-223	10m	F	DIG	L-frontal
08-99	1y3m	F	DIG	L-temporal
09-47	18y	M	PXA	Cerebral cortex
09-49	7y	F	PXA	Parietal
09-78	36y	F	PXA	L-temporal
02-168	10y	F	PXA with neuronal differentiation	R-lateral ventricle
06-232B	23y	M	AT/RT evolving from PXA	R-frontal
08-308B	8y	F	AT/RT evolving from PXA	R-frontal

Abbreviations: M, male; F, female; GG, ganglioglioma; DNT, dysembryoplastic neuroepithelial tumor; GBM, glioblastoma multiforme; DIG, desmoplastic infantile ganglioglioma; PXA, pleomorphic xanthoastrocytoma; AT/RT, atypical teratoid/rhabdoid tumor.

part of 9p, homozygous loss of 9p21.2-21.3, and heterozygous losses of 22q and 19q. One of the 2 samples with a homozygous deletion of 9p21.3 (*CDKN2A/B*) also had loss of 22q. A summary of the array results is graphically displayed in Fig. 2. Detailed breakpoints are shown in Supplementary Material, Table S1.

None of the array results were suggestive of a 7q34 duplication. In order to rule out a cryptic *BRAF* fusion gene, 12 samples with adequate RNA were screened for the common *KIAA1549-BRAF* fusion. The primers for RT-PCR are located in exon 4 of *KIAA1549* and exon 16 of *BRAF*, and thus will detect all of the 5 previously described *KIAA1549-BRAF* fusion products.^{3,4} All 12 samples were negative for all 5 fusion products. In addition, 18 samples with available DNA only were screened using genomic primers located in intron 16 of *KIAA1549* and intron 8 of *BRAF*. All were negative,

although all variant fusion sequences may not be detected with this set of primers (data not shown).

Screening for the 2 common activating mutations in *BRAF* was then performed. DNA sequence analyses for exons 11 and 15 from the 31 tumors did not reveal any case with an exon 11 mutation. Analysis of exon 15 sequence, however, yielded 14 of 31 tumors with a *BRAF* V600E mutation, including 6 GGs, 2 GGs with a prominent astrocytic component, 1 GG with an anaplastic glial component, 1 AT/RT evolving from a GG, 1 DIG, 1 PXA, and 2 AT/RTs evolving from PXAs. DNA isolated from peripheral blood samples from 5 of 14 patients whose tumors had *BRAF* mutations was tested to rule out a germline mutation, and all were negative.

Three AT/RTs evolving from either a GG or PXA had a V600E mutation. The rhabdoid components of these 3 tumors were all shown to demonstrate *INI1*

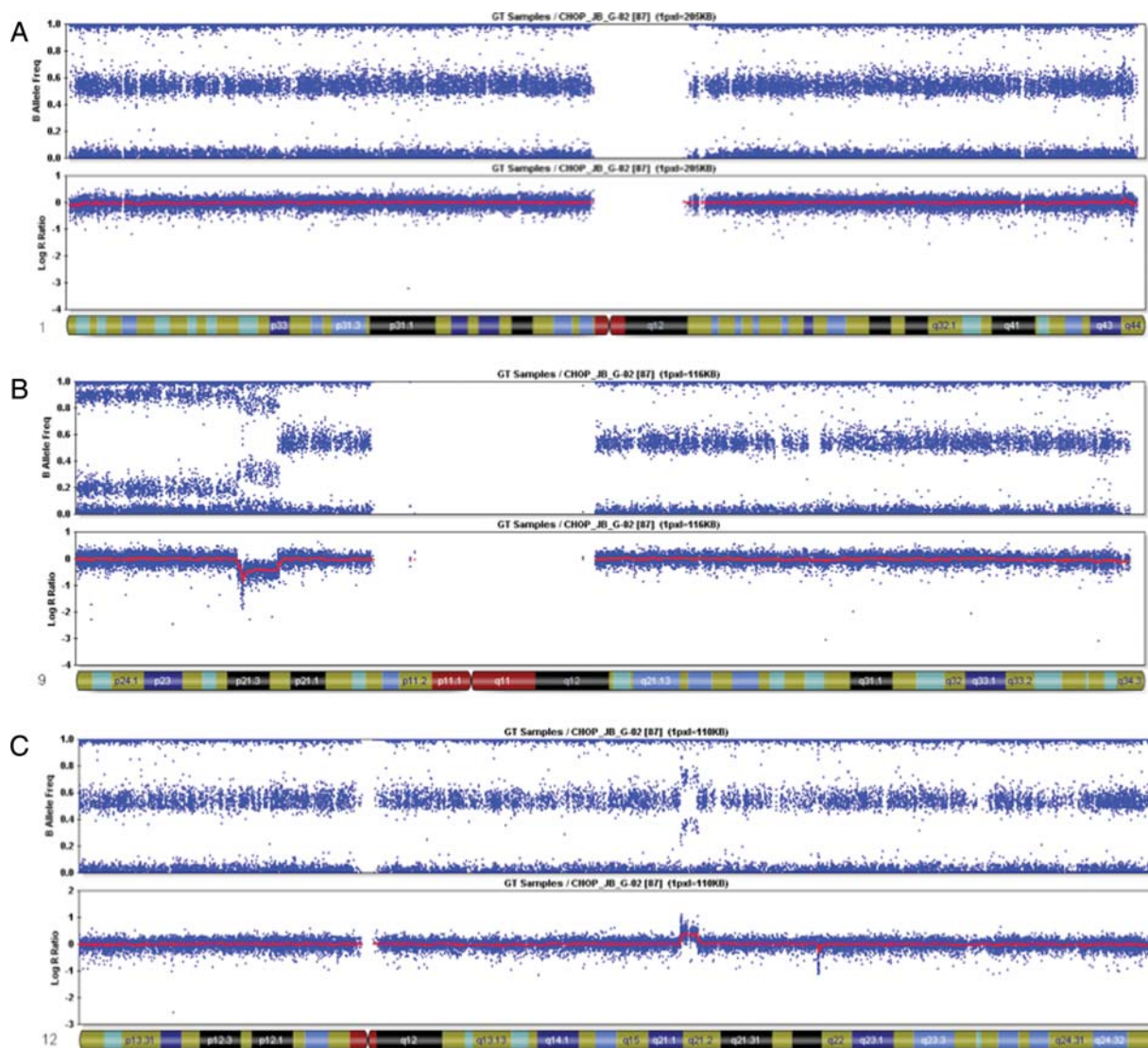


Fig. 1. Illumina BeadStudio results for case 04-234. (A) Chromosome 1 shows a split in the B allele frequency and increase in the log R ratio at 1q44 consistent with a duplication. (B) Chromosome 9 shows a number of abnormalities. At 9p21.3-pter there is a normal log R ratio with a split in the B allele frequency consistent with a CN LOH. There is also a significant decrease in the log R ratio consistent with a homozygous deletion at 9p21.3. At 9p21.3-21.2, the log R ratio is decreased and the B allele frequency is split, consistent with a heterozygous deletion. (C) Chromosome 12 shows a split in the B allele frequency and an increase in the log R ratio at 12q21.1-21.2. A small deletion in 12q21.33 is a normal population variant.

mutations characteristic of AT/RTs.^{36,37} A series of 10 primary AT/RTs was therefore screened for activating *BRAF* mutations in exons 11 and 15. Although each of the 10 AT/RTs screened had biallelic inactivating mutations or deletions of *INI1* leading to loss of *INI1* expression by IHC, none had abnormal exon 11 or 15 *BRAF* sequences (data not shown). *INI1* IHC for the other glioma samples with loss of 22q (05-253, 06-223, and 08-247) was also performed. All 3 cases showed retained *INI1* expression, ruling out an early progression to AT/RT.

Progression to malignancy is often associated with acquisition of a *TP53* mutation or retained staining by IHC.^{18,31} Immunohistochemistry was performed for

p53 in 26 samples (Supplementary Material, Table S2). Nine tumors with expression levels categorized as grade 2 (8 cases) or 3 (case 06-107) were screened for mutations in exons 2–9, but there were no mutations identified. As *IDH1* and *KRAS* have been implicated in the development of low-grade gliomas in adults, mutation screening was performed for the common mutations in these 2 genes. Twelve *BRAF*-negative tumors were screened for an exon 2 or 3 mutation in *KRAS*, and none of the samples had a mutation. Only 1 of 23 samples with adequate DNA, 05-22, had a mutation in *IDH1* exon 4 (data not shown).

Mutations in *BRAF* are predicted to result in activation of the downstream signaling pathway, resulting

Table 2. SNP array results and *BRAF* mutation status for the 33 tumors

Patient ID	Diagnosis	Array gain	Array loss	V600E mutation
00-317	GG	5q35.1, 7, 11q12.2	4p16.1, Xq27.2	–
00-352	GG	2p21	16q23.1	n/a
01-29	GG	–	16p13.2, 20q13.33, Xq25	+
02-145	GG	–	–	–
03-126	GG	–	–	+
04-168	GG	–	18q21.32	+
05-97	GG	–	4q26, 8q12.3-13.1	–
07-304	GG	9p22.1	–	–
07-350	GG	3, 6, 8, 9, 10p14, 12, 16, 17, 18, 19, 22, X	–	+
08-113	GG	7	–	+
08-247	GG	–	9, 9p21.2-21.3 (hmz del), 22q	–
09-127	GG	6, 7, 11	–	+
00-301	GG with prominent pilocytic astrocytoma	–	–	–
02-03	GG with prominent astrocytic component	–	5q35.2-35.3	–
04-234	GG with prominent astrocytic component	12q21.1-21.2	1q44, 9p21.3-pter ^a , 9p21.2-21.3, 9p21.3 (hmz del)	+
05-22	GG with prominent astrocytic component	7, 17p13.1-pter, Xq11.4	7p21.1, 19q	–
06-91	GG with prominent astrocytic component	–	6p21.1, 20p12.1	+
05-253	GG with anaplastic glial component	5p, 7q	22q	+
06-107	GBM arising in a GG	1q, 3q26.1-qter, 7p, 7q11.1-31.31, 17q11.2-qter	3q25.31-26.1, 7q31.31-qter, 8q23.3, 12p12.1-pter	–
04-119	AT/RT evolving from a GG	n/a	n/a	+
00-358	GG/DNT	–	2p12	–
01-44	GG/DNT	–	–	–
95-56	DNT	1p11.1-34.3, 1q, 2p11.1-23.3, 2q, 3p21.31-pter, 3q24-26.31, 5p11-12, 5q11.1-35.2, 6, 8p11.21-11.23, 8q13.1-13.3, 8q21.11, 8q24.13-qter, 9p, 11q12.1-qter, 13, 16p12.2-pter, 17q, 18, 19p, 20	7p12.3-15.3, 8p12-23.1, 8p23.1-pter, 8q22.1, 9q, 10q23.1, 10q24.1-26.1, 12 ^a , 14, 17p12-pter, 19q	n/a
01-206	DNT	–	–	–
05-137	DNT	–	–	–
06-223	DIG	–	9, 22q	–
08-99	DIG	–	–	+
09-47	PXA	n/a	n/a	–
09-49	PXA	n/a	n/a	–
09-78	PXA	n/a	n/a	+
02-168	PXA with neuronal differentiation	–	2q31.2, 9p21.2-pter, 15q21.2, 19q13.41, Xp22.11-q11.2, Xq21.33-qter	–
06-232B	AT/RT evolving from PXA	n/a	n/a	+
08-308B	AT/RT evolving from PXA	n/a	n/a	+

^aCopy number neutral loss of heterozygosity (CN LOH). Abbreviations: GG, ganglioglioma; DNT, dysembryoplastic neuroepithelial tumor; GBM, glioblastoma multiforme; DIG, desmoplastic infantile ganglioglioma; PXA, pleomorphic xanthoastrocytoma; AT/RT, atypical teratoid/rhabdoid tumor; n/a, not performed.

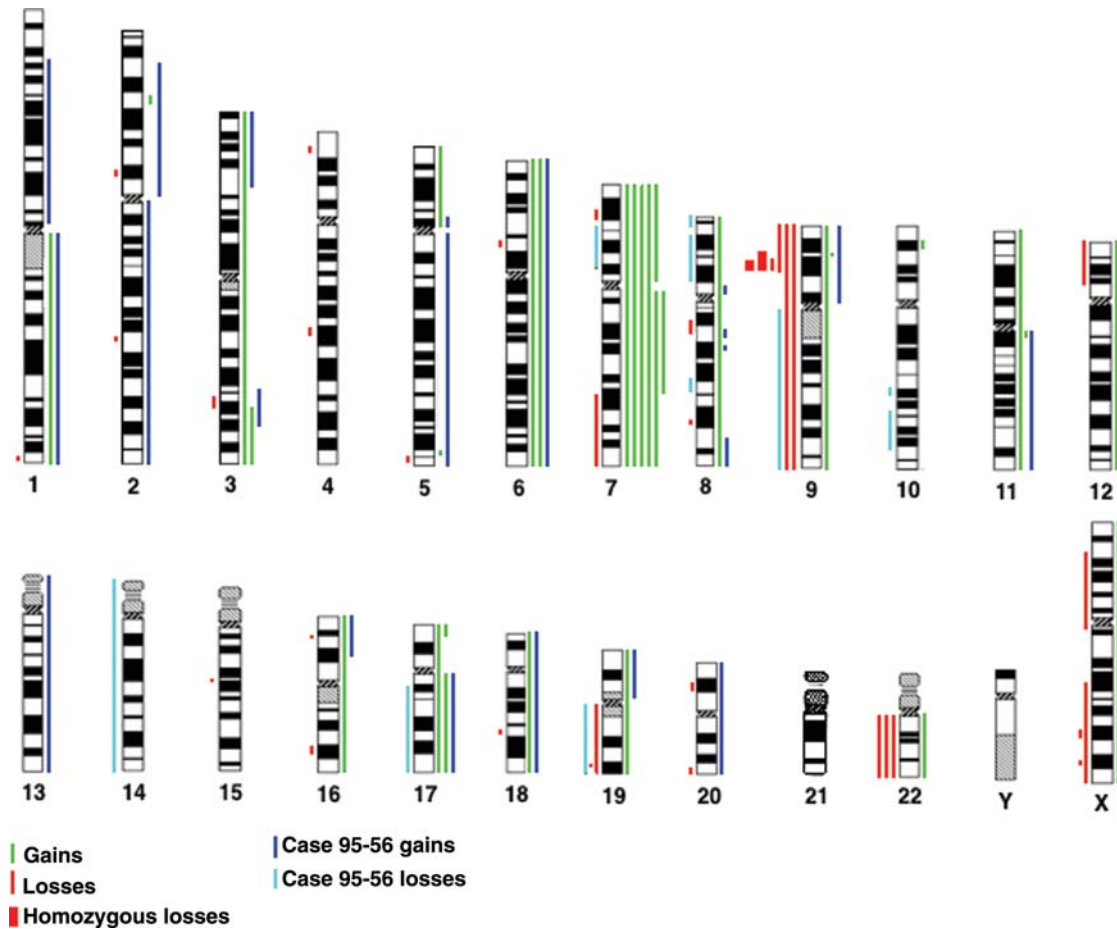


Fig. 2. Summary of chromosomal abnormalities in 20 tumors detected by SNP array analysis. Results for case 95-56 have been shown separately due to the large number of abnormalities detected.

in phosphorylation of MEK1/2, which then phosphorylate the ERK proteins. In order to determine the functional consequences of *BRAF* mutations in this series of tumors, we performed IHC for phospho-ERK. As shown in Fig. 3, a variable pattern of expressivity of phospho-ERK was detected in the tumors with and without *BRAF* mutations. As a group, the tumors with *BRAF* mutations had less intense staining than the comparable group of tumors containing wild-type *BRAF* (data not shown). The tumors with the most intense level of staining were those with prominent glial components, particularly the PXA, the 2 DIGs, 1 GG/DNT and some of the GGs (data not shown). The staining was predominantly cytoplasmic in the astrocytes. The neuronal/ganglion component was negative (Fig. 3; C and D insets). These results suggest that ERK activation is not a specific indicator of *BRAF* activation in tumors. As has been demonstrated in other tumors (eg, melanoma), constitutive *BRAF* activation fails to consistently correlate with phospho-ERK staining. Furthermore, there are likely other mechanisms that may result in MAPK activation in tumors, as evidenced by the phospho-ERK staining in samples without *BRAF* alterations.

Discussion

The present study was undertaken with the aim of further elucidating the molecular etiology of GGs and histologically related low-grade gliomas. DNA from frozen tissue for 27 tumors was analyzed using the Illumina 610K SNP-based oligonucleotide array. Seven of the tumors analyzed had no significant CNAs, and none of the samples had the 7q34 duplication frequently seen in low-grade astrocytomas.² In contrast, the CNAs seen most often in the present study were a gain of chromosome 7, partial loss of 9p that included the *CDKN2A/B* locus, and loss of 19q and 22q. Each of these abnormalities has been reported as a non-random finding in childhood and adult malignant gliomas, and thus may signify a greater likelihood for progression. One case, 95-56, appeared to be an outlier with 21 gains and 11 losses. Unfortunately there was insufficient DNA for mutation analysis and clinical follow-up was not available.

Based on our preliminary studies in which we identified a *BRAF* mutation in 3 GGs, we screened a total of 31 tumors for activating mutations in exons 11 and 15. A single amino acid substitution at position 600 was

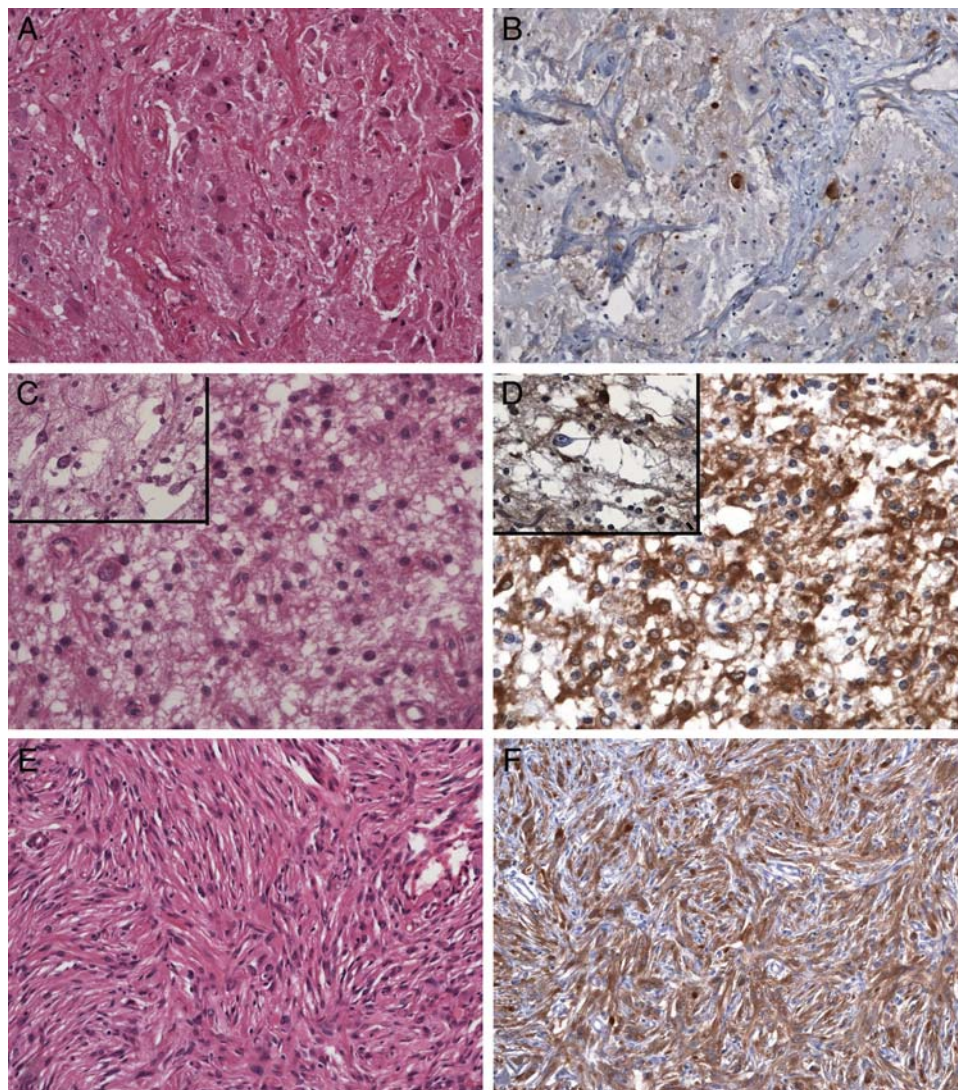


Fig. 3. Immunohistochemical expression of p-ERK in tumors with and without a *BRAF* mutation. GG case 05-253 (A) has a *BRAF* mutation, however p-ERK (B) is expressed only in the cytoplasm of rare neoplastic cells. In contrast, GG/DNT case 00-358 (C) without a *BRAF* mutation, demonstrates diffuse cytoplasmic expression of p-ERK only in the glial component (D) while the "free floating" neurons are negative (inset). Similarly, DIG case 06-223 (E) without a *BRAF* mutation, is strongly and diffusely reactive for p-ERK (F). A, B, E, and F magnification x200, C and D magnification x400, insets magnification x600.

detected in 14 of the 31 tumors analyzed. There did not seem to be any correlation between the CNAs identified by the SNP array analysis and a *BRAF* mutation. Although 3 GGs with the V600E mutation had a gain of all or part of chromosome 7, this gain was also seen in 2 tumors without the mutation. Similarly, 2 tumors had a homozygous deletion of 9p21 (*CDKN2A/B*). One of these tumors had the mutation and the other did not. Interestingly, Forshev et al.⁴ also found 1 fibrillary astrocytoma with a 9p deletion and *BRAF* V600E mutation as well as 1 PXA with loss of 9p, gain of 7, and a *BRAF* V600E mutation. In contrast, 4 DNTs and GG/DNTs in the present cohort had no significant CNAs, and no *BRAF* mutation. Studies with longer clinical follow-up will be useful in determining if there is any correlation between histology, *BRAF* mutation, deletion of *CDKN2A/B* or gain of chromosome 7, and outcome.

Selected tumors in this series were also screened for mutations in *IDH1*, *KRAS*, and *TP53*. None of the tumors had mutations in exons 2 or 3 of *KRAS* or exons 2–9 of *TP53*. Only 1 tumor, 05-22, had a R132H mutation in *IDH1*. Further studies are required to determine the role of *IDH1* in the development of brain tumors in the younger age groups.

In the present study, 9 of 18 GGs (including the 3 previously reported by Sievert et al.²) and 1 of 2 DIGs had the V600E mutation. Three AT/RTs that evolved from either a GG or PXA had the mutation, as did the tumor, 06-91, that recurred 6 months after the initial surgical resection. While this suggests that an activating *BRAF* mutation in a GG or PXA could be a poor prognostic indicator, a *BRAF* mutation alone cannot be associated with poor outcome, given the frequency of *BRAF* mutations present in this group of tumors, and

the relatively good prognosis associated with these diagnoses. In contrast, AT/RTs are specifically associated with *INI1* deletions or mutations and carry a very poor prognosis. While the vast majority of tumors present as primary malignancies, we have now described 3 AT/RTs that arose in the setting of a low-grade tumor with a *BRAF* mutation. While *BRAF* mutations alone do not appear to lead to the development of AT/RT, additional case reports may suggest an increased risk for specific malignancies in this setting.

Although this study was not designed to generate clinical correlative outcome results, we did attempt to collect follow-up data for this series of patients. Limited data were available for 24 of the 33 patients participating in this study. Of these 24, all were still alive at last follow-up (data not shown), although the average time for follow-up was only 3 years. Additional cases with extended follow-up time are needed to correlate the primary and secondary molecular alterations in tumors with malignant transformation, clinical progression, and outcome. Similarly, although none of the patients tested had germline *BRAF* mutations, as these studies are still in their infancy, it remains to be seen whether patients with germline RAS/MAPK pathway mutations, in addition to *NF1*, may be predisposed to glial tumors.

Immunohistochemical analysis of phospho-ERK suggested activation of the RAF-ERK pathway, at least focally, in almost all of the tumors. There was, however, a great deal of variability from diffuse and strong staining, mainly seen in the PXA, 1 DIG, and 2 GGs, to more focal staining, seen in 1 GG/DNT and 2 GGs. Surprisingly, 4 GGs with the mutation demonstrated minimal reactivity. None showed staining of the ganglion/neuronal component stain with this p-ERK antibody.

In this small series of cases, therefore, the staining did not correlate with the presence of a *BRAF* mutation. This phenomenon has also been noted in melanocytic nevi,⁴³ where only 23% of *BRAF* mutated tumors show phospho-ERK activity. This has been hypothesized to result from transient or low level activation of the pathway or a negative feedback loop in *BRAF* V600E mutated tumors.⁷ Alternatively, the positive phospho-ERK staining may reflect a more rapidly proliferating tumor. These studies suggest that activation of other proteins in the RAS-RAF-MEK pathway may result in phosphorylation of ERK and subsequent

downstream signaling in a wide spectrum of grade I and grade II gliomas.

While it is clear from these results that *BRAF* mutations are a major genetic alteration in this histologic group of pediatric brain tumors, further studies are required to clarify the role of *BRAF* activation in their development. If gliomas are similar to melanoma, the expectation is that the V600E mutation alone is not sufficient for the formation of malignant lesions and that additional genetic aberration is required for progression. In fact, a recent study has shown that *PTEN* loss is necessary for the development of malignant melanoma in mice with expression of *BRAF*^{E600}.⁴⁴ Loss of chromosome 10, which contains the *PTEN* locus, was not detected in any of the tumors; however, a full *PTEN* mutation analysis has not been performed. It has been shown that silencing of the *BRAF*^{E600} mutant in an established tumor inhibits further tumor progression and can even result in complete tumor regression.⁷ Targeting the earliest lesion may thus be a successful therapeutic strategy. Clinical trials targeting multiple members of the RAF-MAPK pathway are in progress. Based on the mutation and IHC results presented herein, we suggest that a large percentage of children with varying histologic subtypes of low-grade glioma may benefit from biologically targeted inhibitors of this pathway.

Supplementary Material

Supplementary Material is available at *Neuro-Oncology* online.

Acknowledgements

The authors thank Dr. Marc Rosenblum and Dr. Elisabeth Rushing for contributing cases to this study, and Dr. Arupa Ganguly and Christina Bisacchino for providing primers and help with *TP53* sequencing.

Conflict of interest statement: None declared.

Funding

These studies were supported by a grant from the NIH (CA133173).

References

- Louis DN, Ohgaki H, Wiestler OD, Cavenee WK, eds. WHO Classification of Tumors of the Central Nervous System. Lyon: IARC; 2007.
- Sievert AJ, Jackson EM, Gai X, et al. Duplication of 7q34 in pediatric low-grade astrocytomas detected by high-density single nucleotide polymorphism-based genotype arrays results in a novel *BRAF* fusion gene. *Brain Pathol.* 2008; doi: 10.1111/j1750-3639.2008.00225.x.
- Jones DTW, Kocalkowski S, Liu L, et al. Tandem duplication producing a novel oncogenic *BRAF* fusion gene defines the majority of pilocytic astrocytomas. *Cancer Res.* 2008;68:8673–8677.
- Forshew T, Tatvossian RG, Lawson ARJ, et al. Activation of the ERK/MAPK pathway: a signature genetic defect in posterior fossa pilocytic astrocytomas. *J Pathol.* 2009; doi: 10.1002/path.2558.
- Peyssonaux C, Eychene A. The Raf/MEK/ERK pathway: new concepts of activation. *Biol Cell.* 2001;93:53–62.
- Davies H, Bignell GR, Cox C, et al. Mutations of the *BRAF* gene in human cancer. *Nature.* 2002;417:949–954.
- Michaloglou C, Vredeveld LCW, Mooi WJ, Peepers DS. *BRAF*^{E600} in benign and malignant human tumours. *Oncogene.* 2008;27:877–895.

8. Samuels IS, Saitta SC, Landreth GE. MAP'ing CNS development and cognition: an ERKsome process. *Neuron*. 2009;61:160–168.
9. Choong K, Freedman MH, Chitayat D, et al. Juvenile myelomonocytic leukemia and Noonan syndrome. *J Pediatr Hematol Oncol*. 1999;21:523–527.
10. Feingold M. Costello syndrome and rhabdomyosarcoma (letter). *J Med Genet*. 1999;36:582–583.
11. Burger P, Scheithauer B, eds. AFIP Atlas of Tumor Pathology. Washington, DC: American Registry of Pathology; 2007.
12. Chan CH, Bittar RG, Davis GA, Kalnins RM, Fabinyi GC. Long-term seizure outcome following surgery for dysembryoplastic neuroepithelial tumor. *J Neurosurg*. 2006;104:62–69.
13. Hirose T, Scheithauer BW. Mixed dysembryoplastic neuroepithelial tumor and ganglioglioma. *Acta Neuropathol*. 1998;95:649–654.
14. Prayson RA, Khajavi K, Comair YG. Cortical architectural abnormalities and MIB1 immunoreactivity in gangliogliomas: a study of 60 patients with intracranial tumors. *J Neuropathol Exp Neurol*. 1995;54:513–520.
15. Shimbo Y, Takahashi H, Hayano M, Kumagai T, Kameyama S. Temporal lobe lesion demonstrating features of dysembryoplastic neuroepithelial tumor and ganglioglioma: a transitional form? *Clin Neuropathol*. 1997;16:65–68.
16. Yin X, Hui AB, Pang JC, Poon WS, Ng H. Genome-wide survey for chromosomal imbalances in ganglioglioma using comparative genomic hybridization. *Cancer Genet Cytogenet*. 2002;134:71–76.
17. Hoischen A, Ehrler M, Fassunke J, et al. Comprehensive characterization of genomic aberrations in gangliogliomas by CGH, array-based CGH, and interphase FISH. *Brain Pathol*. 2008;18:326–337.
18. Pandita A, Balasubramaniam A, Perrin R, Shannon P, Guha A. Malignant and benign ganglioglioma: a pathological and molecular study. *Neuro Oncol*. 2007;9:124–134.
19. Sawyer JR, Roloson GJ, Chadduck WM, Boop FA. Cytogenetic findings in a pleomorphic xanthoastrocytoma. *Cancer Genet Cytogenet*. 1991;55:225–230.
20. Yin X, Hui AB, Lion EC, Ding M, Chang AR, Ng H. Genetic imbalances in pleomorphic xanthoastrocytoma detected by comparative genomic hybridization and literature review. *Cancer Genet Cytogenet*. 2002;132:14–19.
21. Weber RG, Hoischen A, Ehrler M, et al. Frequent loss of chromosome 9, homozygous *CDKN2A/p14^{ARF}/CDKN2B* deletion and low *TSC1* mRNA expression in pleomorphic xanthoastrocytomas. *Oncogene*. 2007;26:1088–1097.
22. Bhattacharjee MB, Armstrong DD, Vogel H, Cooley LD. Cytogenetic analysis of 120 primary pediatric brain tumors and literature review. *Cancer Genet Cytogenet*. 1997;97:39–53.
23. Kros JM, Delwel EJ, de Jong THR, et al. Desmoplastic infantile astrocytoma and ganglioglioma: a search for genomic characteristics. *Acta Neuropathol*. 2002;104:144–148.
24. Roberts P, Chumas PD, Picton S, Bridges L, Livingstone JH, Sheridan E. A review of the cytogenetics of 58 pediatric brain tumors. *Cancer Genet Cytogenet*. 2001;131:1–12.
25. Platten M, Meyer-Puttlitz B, Blümcke I, et al. A novel splice site associated polymorphism in the tuberous sclerosis 2 (*TSC2*) gene may predispose to the development of sporadic gangliogliomas. *J Neuropathol Exp Neurol*. 1997;56:806–810.
26. Becker AJ, Löbach M, Klein H, et al. Mutation analysis of *TSC1* and *TSC2* genes in gangliogliomas. *Neuropathol Appl Neurobiol*. 2001;27:105–114.
27. Balss J, Meyer J, Mueller W, Korshunov A, Hartmann C, von Deimling A. Analysis of the *IDH1* codon 132 mutation in brain tumors. *Acta Neuropathol*. 2008;116:597–602.
28. Hartmann C, Meyer J, Balss J, et al. Type and frequency of *IDH1* and *IDH2* mutations are related to astrocytic and oligodendroglial differentiation and age: a study of 1,010 diffuse gliomas. *Acta Neuropathol*. 2009; advance online publication.
29. Korshunov A, Meyer J, Capper D, et al. Combined molecular analysis of *BRAF* and *IDH1* distinguishes pilocytic astrocytoma from diffuse astrocytoma. *Acta Neuropathol*. 2009;118:401–405.
30. Yan H, Parsons DW, Jin G, et al. *IDH1* and *IDH2* mutations in gliomas. *N Engl J Med*. 2009;360:765–773.
31. Pollack IF, Finkelstein SD, Woods J, et al. Expression of p53 and prognosis in children with malignant gliomas. *N Engl J Med*. 2002;346:420–427.
32. Felix CA, Slavic I, Dunna M, Strauss EA, Biegel JA. Germline and somatic p53 gene mutations in pediatric brain tumors. *Med Pediatr Oncol*. 1995;25:431–436.
33. Basto D, Trovisco V, Lopes JM, et al. Mutation analysis of B-RAF gene in human gliomas. *Acta Neuropathol*. 2005;109:207–210. Epub 2004 Nov 17.
34. Basto D, Trovisco V, Lopes JM, et al. Mutation analysis of B-RAF gene in human gliomas. *Acta Neuropathol*. 2005;109:207–210.
35. Knobbe CB, Reifemberger J, Reifemberger G. Mutation analysis of the Ras pathway genes *NRAS*, *HRAS*, *KRAS*, and *BRAF* in glioblastomas. *Acta Neuropathol*. 2004;108:467–470.
36. Chacko G, Chacko AG, Dunham CP, Judkins AR, Biegel JA, Perry A. Atypical teratoid/rhabdoid tumor arising in the setting of a pleomorphic xanthoastrocytoma. *J Neurooncol*. 2007;84:217–222.
37. Allen JC, Judkins AR, Rosenblum MK, Biegel JA. Atypical teratoid/rhabdoid tumor evolving from an optic pathway ganglioglioma: case study. *Neuro Oncol*. 2006;8:79–82.
38. Peiffer DA, Gunderson KL. SNP-CGH technologies for genomic profiling of LOH and copy number. *Clin Lab Int*. 2006 May.
39. Peiffer DA, Le JM, Steemers FJ, et al. High-resolution genomic profiling of chromosomal aberrations using Infinium whole-genome genotyping. *Genome Res*. 2006;16:1136–1148.
40. Di Fiore F, Blanchard F, Charbonnier F, et al. Clinical relevance of *KRAS* mutation detection in metastatic colorectal cancer treated by Cetuximab plus chemotherapy. *Br J Cancer*. 2007;96:1166–1169.
41. Wojcik P, Kulig J, Okon K, et al. *KRAS* mutation profile in colorectal carcinoma and novel mutation—internal tandem duplication in *KRAS*. *Pol J Pathol*. 2008;58:93–96.
42. Nichols KE, Heath JA, Friedman D, et al. *TP53*, *BRCA1*, and *BRCA2* tumor suppressor genes are not commonly mutated in survivors of Hodgkin's disease with second primary neoplasm's. *J Clin Oncol*. 2003;21:4505–4509.
43. Uribe P, Andrade L, Gonzalez S. Lack of association between *BRAF* mutation and MAPK ERK activation in melanocytic nevi. *J Invest Dermatol*. 2006;126:16–166.
44. Dankort D, Curley DP, Carlidge RA, et al. *Braf^{V600E}* cooperates with *Pten* loss to induce metastatic melanoma. *Nat Genet*. 2009;41:544–552.